

1 **Supplementary Information**

2
3 **Development of an accurate “composition-process-properties” dataset for**
4 **SLMed Al-Si-(Mg) alloys and its application in alloy design**

5 **Tianchuang Gao¹, Jianbao Gao^{1,*}, Jinliang Zhang², Bo Song², Lijun Zhang^{1,*}**

6
7 ¹State Key Laboratory of Powder Metallurgy, Central South University, Changsha
8 410083, Hunan, China

9 ²State Key Laboratory of Materials Processing and Die & Mould Technology,
10 Huazhong University of Science and Technology, Wuhan 430074, Hubei, China

11
12 ***Correspondence to:** Dr. Jianbao Gao, State Key Laboratory of Powder Metallurgy,
13 Central South University, Lushannan Road No. 932, Changsha 410083, Hunan, China.
14 E-mail: jianbao.gao@csu.edu.cn; Prof. Lijun Zhang, State Key Laboratory of Powder
15 Metallurgy, Central South University, Lushannan Road No. 932, Changsha 410083,
16 Hunan, China. E-mail: lijun.zhang@csu.edu.cn

17
18 **ORCID:** Jianbao Gao(0000-0002-8838-8681);Lijun Zhang(0000-0002-8838-8681)

19
20
21 **Table S1.** The statistical results (range, mean, and standard deviation) of the
22 concentration of each element, Ed, rotation angle, tensile direction, UTS, YS, and EL
23 among the 167 data before data cleaning.

	W(Si) (wt%)	W(Mg) (wt%)	Ed (J/mm ³)	Rotation (°)	Direction (°)	UTS (MPa)	YS (MPa)	EL (%)
count	176	176	176	176	176	176	176	176
mean	9.62	0.27	56.62	74.26	25.06	373.56	239.63	7.33
std	2.19	0.22	27.07	12.31	40.45	68.36	56.17	4.61
min	4.07	0.00	13.33	45.00	0.00	185.20	103.00	0.54
25%	7.19	0.00	39.99	67.00	0.00	321.13	206.38	3.91
50%	10.00	0.30	50.79	67.00	0.00	385.00	243.40	6.70
75%	11.87	0.46	62.08	90.00	90.00	426.40	287.20	9.15
max	12.47	0.65	176.19	90.00	90.00	514.00	334.00	22.00

24
25
26
27
28 **Table S2.** The statistical results (range, mean, and standard deviation) of the

29 concentration of each element, Ed, rotation angle, tensile direction, UTS, YS, and EL
 30 among the model-constructing data set after data cleaning.

	W(Si) (wt%)	W(Mg) (wt%)	Ed (J/mm ³)	Rotation (°)	Direction (°)	UTS (MPa)	YS (MPa)	EL (%)
count	142	142	142	142	142	142	142	142
mean	9.29	0.31	59.36	72.58	24.72	379.69	237.90	8.36
std	2.19	0.22	27.37	11.88	40.31	67.66	58.34	4.36
min	4.07	0.00	17.92	45.00	0.00	246.00	103	2.40
25%	7.14	0.00	45.55	67.00	0.00	326.43	198.03	5.23
50%	10.00	0.30	52.43	67.00	0.00	390.50	243.40	7.55
75%	10.38	0.55	62.08	90.00	90.00	434.19	290.28	9.88
max	12.47	0.65	176.19	90.00	90.00	514.00	327.00	22.00

31

32

33 **Table S3.** The optimized hyperparameters of MLPReg model.

Hyperparameter	Value
neurons number	(100,200)
activation function	'ReLU'
solver	'L-BFGS'
alpha	0.6
random state	84
tol	0.0001

34

35 The hyperparameters of the MLPReg model were optimized by a random search
 36 strategy with a 10% testing data set. The structure of the optimized MLPReg model
 37 was 5×2×3 (5 input features, 2 hidden layers, and 3 output features), and the number
 38 of neurons in the two hidden layers is 100 and 200, respectively. The rectified linear
 39 unit (ReLU) function is used as the activation function. 'L-BFGS' was used as the
 40 solver for weight optimization. The best combinations of hyperparameters are the
 41 following: 'alpha' = 0.6(strength of the L2 regularization term), 'random state' =
 42 84(determines random number generation for weights and bias initialization), and 'tol'
 43 = 0.0001(tolerance for the optimization).

44 **Table S4.** The experimental data for model accuracy verification, which are

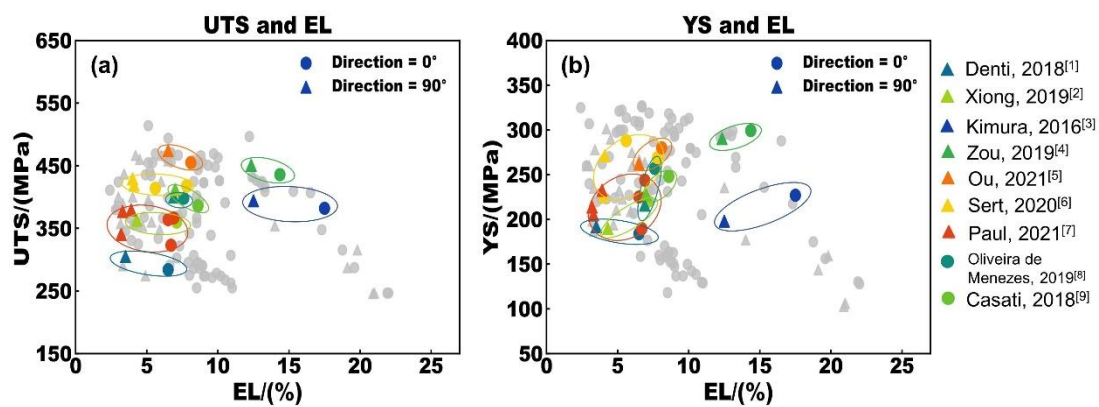
45 unduplicated with the data set used to establish the model.

ID	Alloy	W(Si) (wt%)	W(Mg) (wt%)	Ed (J/mm ³)	Rotation Direction (°)	UTS (MPa)	YS (MPa)	EL (%)
A1	Al-12Si	12.00	0	39.60	79	418.9	220.5	3.91
A2	Al-12Si	12.00	0	39.60	79	369.3	202.2	4.38
A3	Al-12Si	12.00	0	39.99	73	302.7	276.6	2.3
B1	AlSi10Mg	10.81	0.56	80.13	67	384.6	227.3	7.41
B2	AlSi10Mg	10.00	0.30	38.70	67	425	246	9.5
B3	AlSi10Mg	10.00	0.30	38.70	67	402	223	5.7
C1	A357	7.00	0.60	94.35	67	413	222	11
C2	A357	7.04	0.52	60.61	67	427	280	10.5
C3	A357	7.04	0.52	60.61	67	395	232	5.1

46

47

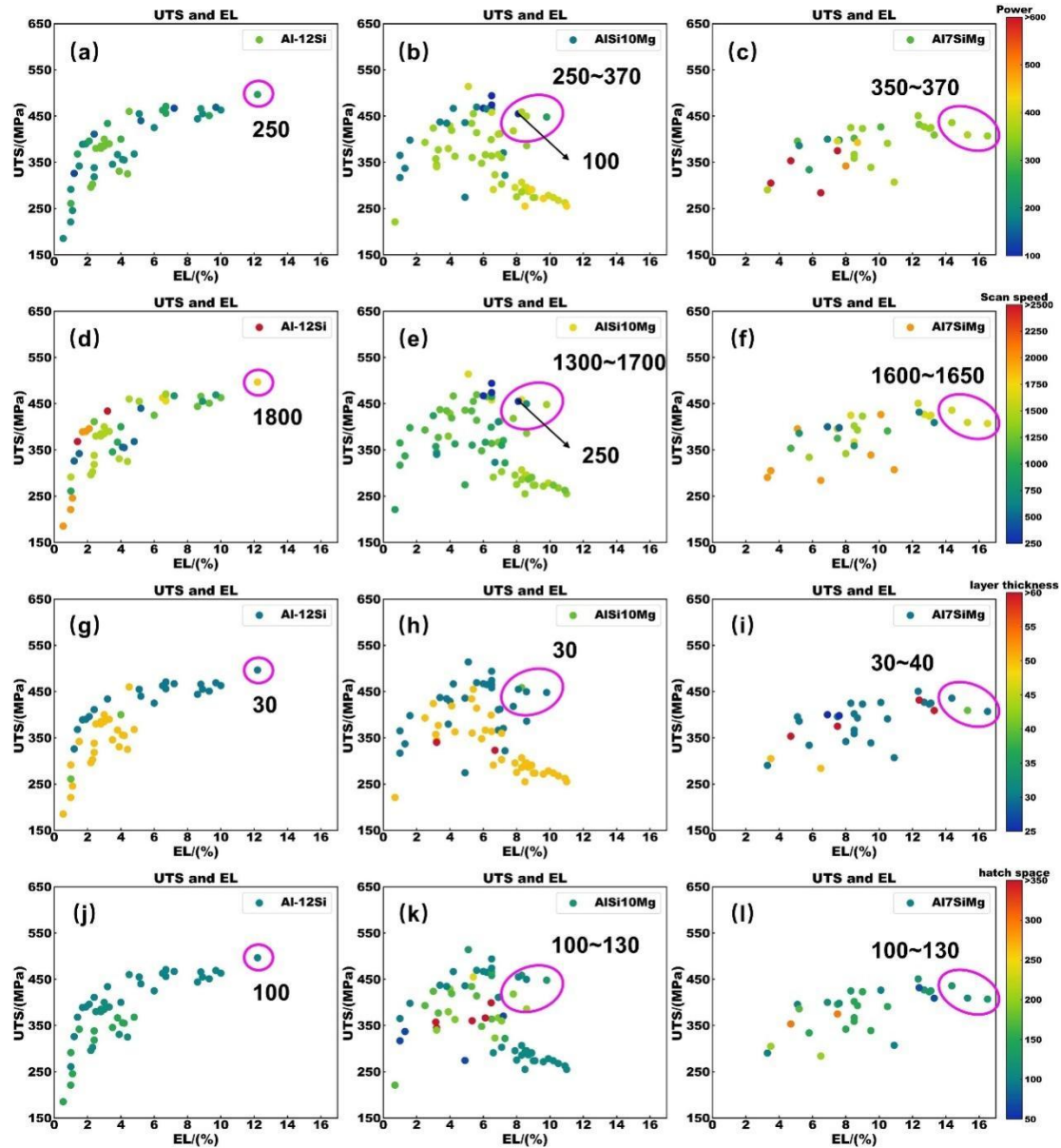
48



49

50 **Figure S1.** The UTS, YS, and EL for the alloys under 0° and 90° test direction,
 51 respectively. Those data points marked by the same color mean that they come from
 52 the same report with the same preparation condition^[1-9].

53



54

55 **Figure S2.** The impact of d laser power, scan speed, hatch space, and layer thickness on
 56 the properties of Al12Si (a, d, g, j), AlSi10Mg (b, e, h, k), and Al7SiMg (c, f, i, l).

57

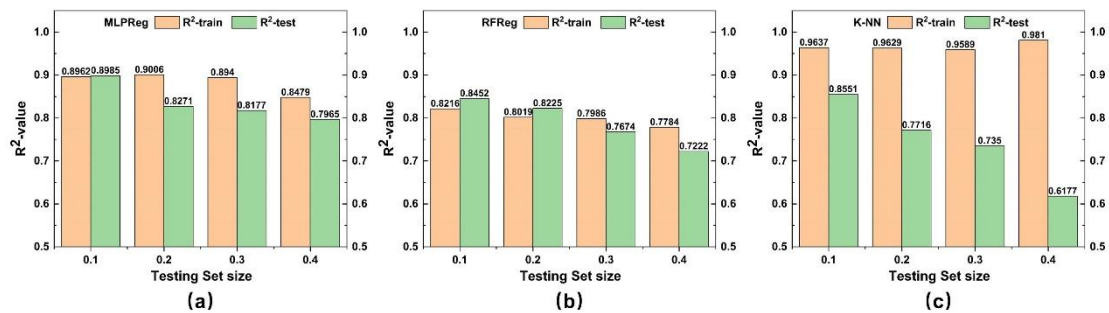
58 **Data analysis**

59

60 Based on the existing experimental data set, the effect of detail manufacturing
 61 parameters (laser power, scan speed, hatch space, and layer thickness) on the
 62 properties of SLMed Al-Si-Mg alloys were further investigated and analyzed. As
 63 shown in **Figure S2 a-f**, high strength and high ductility can be achieved when high
 64 laser power and slow scan speed are applied in Al12Si and AlSi10Mg preparation.
 65 This can be explained by the results of Suzuki's study^[10]. When laser power became
 higher, and scan speed became lower, the energy density and the alloy density

66 increased, the crystal grain size and the fraction of <001> oriented α -Al crystal grains
 67 toward the building direction increased, and the high concentration of solute Si in
 68 α -Al matrix led to good mechanical property. In addition, as can be seen in **Figure S2**
 69 **g-l**, the properties of the alloy are usually lower when the layer thickness and the
 70 hatch space are larger. According to **Eq. 4**, the E_d reduces with the layer thickness and
 71 hatch space increasing. Lower E_d is not conducive to improving the performance of
 72 the alloy. As a result, the optimal layer thickness is 30 μm ~40 μm , and the optimal
 73 hatch space is 100 μm ~130 μm . Laser power can vary from 250 W to 370 W;
 74 correlatedly, the scan speed varies from 1300 mm/s to 1800 mm/s. The optimum laser
 75 power value decreases as the Si content increases, but the optimal scan speed
 76 increases as the Si content increases. For Al7SiMg alloy, the optimal combination of
 77 laser power and scanning speed is 350 W~370 W with 1600 mm/s ~1650 mm/s, but
 78 250 W with 1800 mm/s to Al12Si alloy. In other words, the variation of E_d mainly
 79 depends on laser power and scanning speed.

80
81



82

83 **Figure S3.** R² score of (a) MLPRreg, (b) RFReg, and (c) K-NN, with the size of the
 84 testing set varying from 10% to 40%.

85

86

87 REFERENCE

- 88 1. Denti L. Additive Manufactured A357.0 Samples Using the Laser Powder Bed
 89 Fusion Technique: Shear and Tensile Performance. *Metals* 2018;8:670. [DOI:
 90 10.3390/met8090670].
- 91 2. Xiong ZH, Liu SL, Li SF, et al. Role of melt pool boundary condition in
 92 determining the mechanical properties of selective laser melting AlSi10Mg alloy.
 93 *Mater Sci Eng A* 2019;740–741:148–56. [DOI: 10.1016/j.msea.2018.10.083].

- 94 3. Kimura T, Nakamoto T. Microstructures and mechanical properties of A356
95 (AlSi7Mg0.3) aluminum alloy fabricated by selective laser melting. *Mater Des*
96 2016;89:1294–301. [DOI: 10.1016/j.matdes.2015.10.065].
- 97 4. Zou T, Ou Y, Zhu H, Li L. Effects of Heat Treatment on Microstructure and
98 Tensile Properties of AlSi7Mg Alloy Fabricated by Selective Laser Melting. *Hot*
99 *Work Technol* 2019;48:154–7. [DOI: 10.14158/j.cnki.1001-3814.2019.20.037].
- 100 5. Ou Y, Zhang Q, Wei Y, et al. Evolution of Heterogeneous Microstructure and its
101 Effects on Tensile Properties of Selective Laser Melted AlSi10Mg Alloy. *J Mater*
102 *Eng Perform* 2021;30:4341–55. [DOI: 10.1007/s11665-021-05757-6].
- 103 6. Sert E, Hitzler L, Hafenstein S, et al. Tensile and compressive behaviour of
104 additively manufactured AlSi10Mg samples. *Prog Addit Manuf* 2020;5:305–13.
105 [DOI: 10.1007/s40964-020-00131-9].
- 106 7. Paul MJ, Liu Q, Best JP, et al. Fracture resistance of AlSi10Mg fabricated by laser
107 powder bed fusion. *Acta Mater* 2021;211:116869. [DOI:
108 10.1016/j.actamat.2021.116869].
- 109 8. Oliveira de Menezes JT, Castrodeza EM, Casati R. Effect of build orientation on
110 fracture and tensile behavior of A357 Al alloy processed by Selective Laser
111 Melting. *Mater Sci Eng A* 2019;766:138392. [DOI: 10.1016/j.msea.2019.138392].
- 112 9. Casati R, Hamidi Nasab M, Coduri M, Tirelli V, Vedani M. Effects of Platform
113 Pre-Heating and Thermal-Treatment Strategies on Properties of AlSi10Mg Alloy
114 Processed by Selective Laser Melting. *Metals* 2018;8:954. [DOI:
115 10.3390/met8110954].
- 116 10. Suzuki A, Miyasaka T, Takata N, Kobashi M, Kato M. Control of microstructural
117 characteristics and mechanical properties of AlSi12 alloy by processing
118 conditions of laser powder bed fusion. *Addit Manuf* 2021;48:102383. [DOI:
119 10.1016/j.addma.2021.102383].